Available online at www.sciencedirect.com
SCIENCE DIRECT®
Electrochimica Acta 50 (2005) 5032–5043
ELECTROCHIMICA Acta
www.elsevier.com/locate/electacta

Kinetics of copper deposition on Pt(1 1 1) and Au(1 1 1) electrodes in solutions of different acidities

A.I. Danilov [a,*,1], E.B. Molodkina [a], A.V. Rudnev [a,1], Yu. M. Polukarov [a,1], J.M. Feliu [b,1]

[a] *Institute of Physical Chemistry and Electrochemistry of RAS, Moscow, Russia*
[b] *Institute of Electrochemistry, University of Alicante, Alicante, Spain*

Received 21 December 2004; received in revised form 4 February 2005; accepted 7 February 2005
Available online 29 June 2005

Abstract

Kinetics and mechanism of underpotential (UPD) and overpotential Cu deposition (OPD) on Pt(1 1 1), Pt(7 7 5) and Au(1 1 1) electrodes in sulfate solutions of different acidities (pH 0.3–3.7) are studied. In weakly acid solutions, the rates of both Cu UPD and OPD processes are higher as compared with acid solution of copper sulfate (pH 0.3) due to the enhanced concentration of active centers (copper oxides Cu_xO) for 2-D and 3-D phase transitions and accelerated discharge of copper ions. The maximum rate of $(\sqrt{3} \times \sqrt{3})R30^\circ$ formation is observed at pH 2.7–3.0. At pH > 3.0, the platinum surface is partially blocked by strongly adsorbed oxygen-containing species. At pH < 2.7, the inhibition of Cu UPD and the adlayer desorption are due to the decrease in the charge transfer rate and concentration of copper oxides, which are the defects of adlayer. An optimal, not too high, concentration of adsorbed oxygen-containing species is necessary for ensuring the maximum rate of Cu UPD on platinum. Acidity of electrolytes affects considerably the rate of Cu deposition on Pt(1 1 1) but has only a slight influence on the kinetics of Cu UPD on Au(1 1 1) electrode due to the weaker adsorption of OH^- ions on gold. However, the increase in pH accelerates bulk Cu deposition on Au(1 1 1). Adsorption of sulfate anions and hydroxide ions on a monolayer of copper adatoms and Cu crystallites provides accelerated charge transfer (local electrostatic double layer effects of electronegative species) and probably increases the amount of active centers for 3-D nucleation.

Keywords: Pt(1 1 1); Au(1 1 1); Stepped surfaces; Cu UPD and OPD; pH effects; Active centers

1. Introduction

Kinetics and mechanism of initial stages of copper electrocrystallization on foreign substrates are well documented ([1–9] and references cited therein) due to their fundamental (a suitable model system for studying complicated multistage reactions and phase transitions) and applied importance. Underpotential deposition (UPD) of copper on platinum and gold substrates is the first stage of the process; the kinetics of adlayer formation affects the rates of subsequent three-dimensional nucleation and growth (Stransky–Krastanov mechanism). However, most of publications on this subject are devoted to Cu deposition in acid solutions and only a few of them [10–16] deal with weakly acidic electrolytes (pH > 2).

It is known that small amounts of specifically adsorbed anions accelerate the charge transfer, due to local electrostatic effects in the electric double layer and the process of metals electrodeposition in general ([1–9,13–26] and references cited therein). Copper oxides (Cu_xO or mixed oxides Pt_xCu_yO) formed by a slow surface reaction between coadsorbed oxygen compounds and copper adatoms at potentials 0.5–0.9 V (NHE) exercise similar influence on the rate of copper electrocrystallization on Pt(poly) and Pt(1 1 1) electrodes [13–16,27–31], these species act as the active centers for Cu adlayer formation and subsequent overpotential deposition (OPD). We have come to this conclusion on the basis of electrochemical data on initial stages of copper deposition on platinum in acidic (pH 0.3) and weakly acidic (pH 3.0–3.7)

* Corresponding author. Tel.: +7 095 955 4455; fax: +7 095 952 5308.
E-mail address: danilov@phyche.ac.ru (A.I. Danilov).
[1] ISE member.

0013-4686/$ – see front matter © 2005 Elsevier Ltd. All rights reserved.
doi:10.1016/j.electacta.2005.02.078

sulfate and perchlorate solutions. We consider an active center as a site, in which the nucleation work is smaller or the growth of nucleus is faster.

Cu_2O and CuO should not be considered as thermodynamically stable phases at pH 0.3. However, the results on the adsorption behavior of copper electrodes by surface-enhanced Raman spectroscopy (SERS) in solutions of different acidities [32] could be considered as a spectroscopic proof of the copper oxides existence in acid solutions. Oxygen-containing species on Cu(*h k l*) single crystals were detected under similar conditions by in situ STM [33–35] as well.

Our recent studies of copper electrocrystallization on Pt(1 1 1) were performed in acid sulfate solutions (pH 0.3) [30]. To better understand the mechanism of the process and the role of surface oxides, we have carried out additional investigations of the UPD and bulk Cu deposition on a Pt(1 1 1) electrode in weakly acidic solutions, where the probability of Cu_xO formation is much higher and also on Au(1 1 1) in solutions at pH 0.3 and 3.7, where adsorption of oxygen compounds is lower as compared with Pt. This report presents the results of studies of Cu UPD and OPD in copper sulfate solutions (pH 0.3–3.7), performed for clarifying the kinetics and mechanism of the Cu electrocrystallization on Pt(1 1 1) and Au(1 1 1) electrodes.

2. Experimental

The experiments have been performed with Pt(1 1 1), Pt(7 7 5) and Au(1 1 1) electrodes prepared by Clavilier's method [36–39] (surface areas of ca. 0.04 cm^2). The electrodes were annealed in gas–air flame of Bunsen burner, cooled in air (Pt(1 1 1) and Au(1 1 1)), quenched in Milli-Q water [36,37] and placed in the cell with argon atmosphere above a degassed 0.5 M H_2SO_4 solution. To avoid oxidation of the stepped Pt(7 7 5) surface, the cooling was performed in $Ar + H_2$ mixture. After checking the degree of system purity and the quality of a crystal in sulfuric acid (Fig. 1, curve 1), the electrodes were transferred to the cell with 10 mM $CuSO_4$ + 0.5 M H_2SO_4 (pH 0.3) or 10 mM $CuSO_4 + (0.5 - x)$ M $Na_2SO_4 + x$ M H_2SO_4 (pH 1.0–3.7).

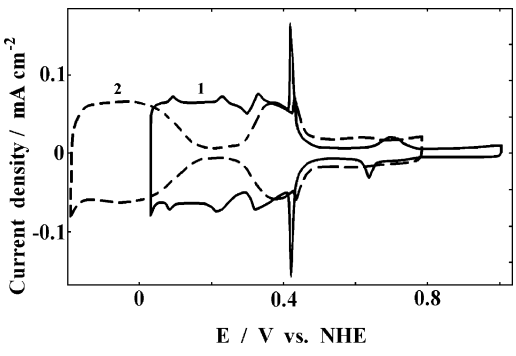

Fig. 1. Steady-state CV profiles of Pt(1 1 1) electrode in solutions of 0.5 M H_2SO_4 (1, pH 0.3) and 0.5 M Na_2SO_4 + 0.5 mM H_2SO_4 (2, pH 3.7) at sweep rate of 0.1 V s^{-1}.

Acidity of the electrolyte was varied during the experiment from pH 3.7 to 2.7 by addition of corresponding aliquots of 0.5 M H_2SO_4 solution directly to the cell.

The three-compartment glass cell, chemicals and electrochemical equipment were described in Ref. [30]. A Hg/Hg_2SO_4 electrode in 0.5 M H_2SO_4, a quasi-reversible Cu/Cu^{2+} electrode in the same Cu-containing solution or a reversible hydrogen electrode in the same Cu-free solution were used as the reference electrode. All potentials in the paper are related to the normal hydrogen electrode (NHE). As a standard polarization procedure, the electrode potential was cycled at a sweep rate of 0.1 V s^{-1}. Using this relatively high rate of potential cycling allows one to control slight changes in the kinetics of slow UPD processes [30], which cannot be detected under steady-state conditions (slow potential cycling). The studies of morphology of copper deposits were performed using a scanning electron microscope JSM-U3 (JOEL Company, Japan) and electrochemical scanning tunneling microscope "Solver Pro EC" (NT-MDT Company, Russia).

3. Results and discussion

3.1. Cyclic voltammetry, Cu UPD on Pt(1 1 1)

Cyclic voltammograms (CV) in 0.5 M H_2SO_4 (pH 0.3) with high reversible peaks at ca. 0.4 V (curve 1 in Fig. 1, phase transitions "order–disorder" [40,41] for adsorbed bisulfate) characterize the high quality of the Pt(1 1 1) electrode with wide (1 1 1) terraces and a low concentration of defects.

In copper-free weakly acidic solution of 0.5 M Na_2SO_4 + 0.5 mM H_2SO_4 (pH 3.7, curve 2 in Fig. 1), the peaks of phase transitions are significantly lower as compared with the acid solution. Similar cyclic voltammograms (CV) were presented in Refs. [42–45]. According to radiochemical data [42], sulfate adsorption is lower in weakly acidic solutions, which means that a certain amount of hydroxide ions are adsorbed on the surface. Probably, these species represent the defects in the ordered adlattice $(\sqrt{3} \times \sqrt{7})R\,19^\circ$ of bisulfate or sulfate ions and the phase transition "order–disorder" proceeds within a wider potential window.

Figs. 2 and 3 show steady-state CV profiles of Pt(1 1 1) electrode in copper sulfate solutions at pH 0.3–3.7. Dynamic cathodic isotherms (curves 1–3 in Fig. 4, absolute values of charge densities are plotted) were obtained by integration of negative-going CV sweeps from 0.7 to 0.25 V without taking into account the double layer charging and adsorption–desorption of anions. These curves allow estimating the changes in the surface coverage by copper adatoms during the deposition, as a first approximation. To estimate steady-state isotherms (curves 4 and 5 in Fig. 4), cyclic voltammetry was combined with potentiostatic polarization at various potentials. After standard pretreatment at 100 mV s^{-1}, the electrode was fixed at a certain potential E_h

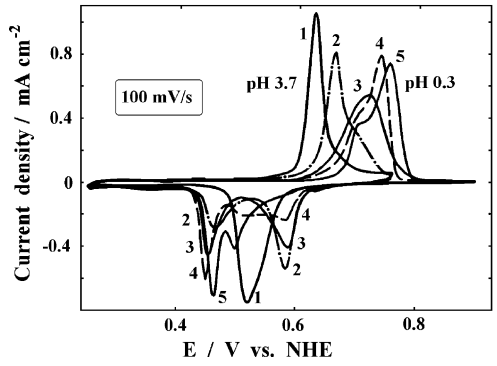

Fig. 2. The steady-state CV profiles of Cu UPD on Pt(1 1 1) electrode in solutions of different acidities at sweep rate of 0.1 V s^{-1}. pH values: 1–3.7; 2–3.0; 3–1.7; 4–1.0; 5–0.3.

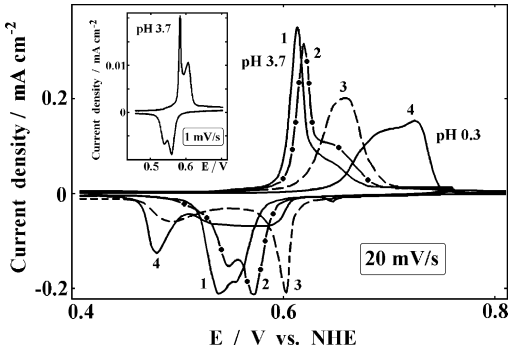

Fig. 3. Fragments of the steady-state CV profiles of Cu UPD on Pt(1 1 1) electrode in solutions of different acidities at sweep rate of 20 mV s^{-1}. pH values: 1–3.7; 2–3.4; 3–2.7; 4–0.3. *Insert:* CV at pH 3.7 and sweep rate of 1 mV s^{-1}.

for 500 s and the current of Cu_{ad} desorption was recorded during the following positive-going sweep from E_h to 1.0 V at pH 0.3 or from E_h to 0.78 V at pH 3.7. The isotherms 4 and 5 in Fig. 4 (Q versus E_h dependencies) have been obtained by integrating of these positive-going sweeps after polarization at E_h (curve 4, filled circles, pH 0.3; curve 5, squares, pH 3.7) without double layer correction.

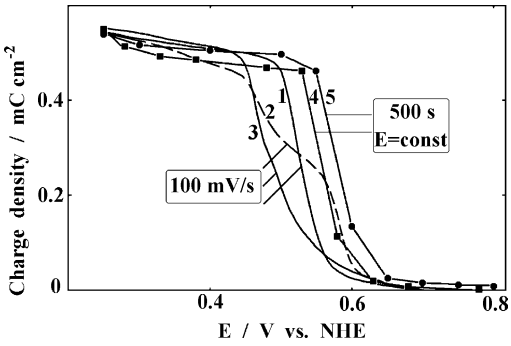

Fig. 4. Dynamic (1–3) and steady-state (4 and 5) isotherms of Cu adsorption on Pt(1 1 1) electrode in solutions of different acidities. pH values: 1.4–3.7; 2–3.0; 3.5–0.3. The explanations are outlined in the text.

We will discuss mainly the data gained at relatively high sweep rates because (i) a full monolayer of Cu is formed at 0.25 V under steady-state conditions at pH 0.3 and 3.7; (ii) the isotherms are similar to one another (curves 4 and 5 in Fig. 4); (iii) information about the kinetics of UPD (it was one of the main goals of this study) can be lost at low potential cycling rates.

In weakly acidic solutions (pH 3.7, curve 1 in Fig. 2) at a sweep rate of 0.1 V s^{-1}, only one peak for copper deposition at ca. 0.5 V and a single peak for Cu_{ad} desorption at ca. 0.62 V are recorded. However, slow potential cycling allows to observe splitting of both anodic and cathodic peaks (Fig. 3), this fact indicates that Cu UPD in this solution is a two-stage process. Probably, the formation of a Cu(1 × 1) monolayer follows the coadsorption of Cu adatoms with anions, just as for Cu UPD on Pt(1 1 1) in acidic solutions and on Au(1 1 1) ([30,46–56] and references cited therein).

The increase in acidity of solutions leads to noticeable changes in the CV profile (Figs. 2 and 3). The splitting of a single cathodic peak (pH 3.7) and the positive shift of the right peak are observed with the decrease in pH at a sweep rate of 0.1 V s^{-1} (Fig. 2). At 0.02 V s^{-1}, the double cathodic peak (pH 3.7, curve 1 in Fig. 3) transforms into a single peak with a left shoulder (pH 3.4, curve 2); at pH 1.0–3.0, two cathodic peaks are observed with separation of ca. 0.1 V (curve 3 in Fig. 3, pH 2.7). These changes in CVs profiles correspond to acceleration of the first UPD stage (positive shift of the right peak) and hindering of the phase transition of Cu(1 × 1) formation from the lattice $(\sqrt{3} \times \sqrt{3})R30°$; the second UPD stage takes place at less positive potentials (curve 2 in Fig. 4) as compared with the UPD process at pH 3.7.

The maximum rate of formation of the coadsorption lattice "adatoms–anions" is observed at pH 2.7–3.0 (the maximum height of cathodic peak at ca. 0.6 V, see curve 2 in Fig. 2, curve 3 in Fig. 3 and curve 2 in Fig. 4, $Q < 0.3$ mC cm^{-2}). The further increase in solution acidity (pH < 2.7) leads to inhibition of this process (cathodic current at $E > 0.55$ decreases, curves 3–5 in Fig. 2, curve 4 in Fig. 3 and curve 3 in Fig. 4), Cu UPD takes place mainly at $E < 0.55$ V. The desorption peak at positive-going potential sweeps shifts to the positive direction with a decrease in pH of solutions. The tendency of pH-induced UPD kinetic changes is the same for sweep rates 0.02–0.10 V s^{-1}.

The rate of phase transition "$(\sqrt{3} \times \sqrt{3})R30°$–Cu(1 × 1)" depends to the great extent on the concentration of defects of the "adatoms–anions" lattice [12,28], which are the active centers for the formation of two-dimensional Cu(1 × 1) islands. The number of defects determines the potential range and rate of adatoms desorption for the anodic process as well. In addition to structural defects, e.g. steps and kink sites [12], the strongly adsorbed OH^- ions and copper oxides Cu_xO, which are formed at the OH^- and Cu_{ad} coadsorption, could be considered as the adlayer defects and active centers.

Another important factor is the rate of charge transfer, it depends on the electrode potential and local electrostatic

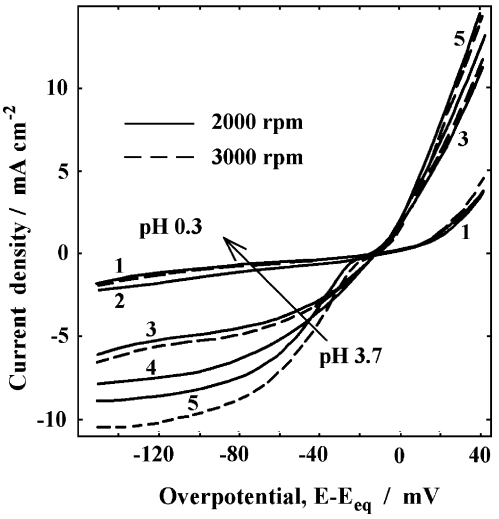

Fig. 5. Polarization curves of copper-covered Pt(poly) rotating disc electrode in solutions of different acidities. pH values: 1–0.3; 2–1.7; 3–2.7; 4–3.0; 5–3.7. Rotation speed of the electrode: 2000 rpm (solid lines) and 3000 rpm (dashed lines for pH 0.3, 2.7 and 3.7). Potential sweep rate is 1 mV s^{-1}.

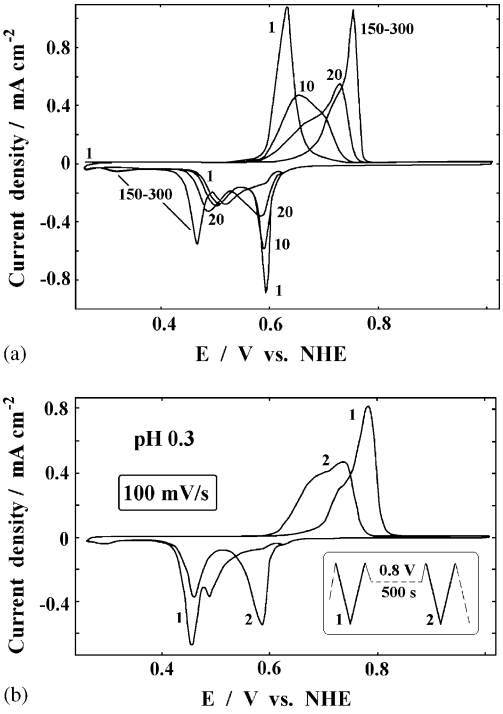

Fig. 6. (a) Initial cycles of Pt(1 1 1) and steady-state CV profile (150–300 cycles) in solution of 0.5 M H_2SO_4 + 10 mM $CuSO_4$ (pH 0.3) after the transfer of the electrode from 0.5 M Na_2SO_4 + 0.5 mM H_2SO_4 + 10 mM $CuSO_4$ (pH 3.7). The digits near the curves correspond to the numbers of consequent cycles. (b) Steady-state CV before (1) and first cycle after (2) potentiostatic polarization of Pt(1 1 1) at 0.8 V for 500 s in the acidic solution (pH 0.3). The sweep rate is 0.1 V s^{-1}. *Insert:* scheme of *E–t* dependence.

effects in electric double layer caused by electronegative oxygen-containing species (anions and oxides) specifically adsorbed on the positively charged Pt surface. Polarization curves in Fig. 5 demonstrate accelerated charge transfer at the discharge-ionization of copper in weakly acidic solutions due to OH^- adsorption (a similar effect we observed in solution of 0.5 M $NaClO_4$ + 1 mM $HClO_4$ + 10 mM $Cu(ClO_4)_2$, pH 3.0 [15]).

A high concentration of copper oxides on platinum is expected at pH 3.7. The data in Fig. 6 can be considered as an evidence of the enhanced amount of active centers on the Pt(1 1 1) surface in weakly acidic solutions. The electrode was quickly transferred from the weakly acidic copper sulfate solution (pH 3.7) to the cell with 0.5 M H_2SO_4 + 10 mM $CuSO_4$ (pH 0.3). Initial cycles demonstrate accelerated Cu deposition (a high cathodic peak at 0.6 V for the $(\sqrt{3} \times \sqrt{3})R30^\circ$ formation) and fast adlayer desorption at $E < 0.7$ V in the presence of copper oxides, which were accumulated on Pt(1 1 1) surface at pH 3.7. The steady-state CV profile can be recorded only upon 20–30 min cycling, after the surface concentration of Cu_xO has been decreased (deactivation of the electrode surface).

A similar active state of the Pt(1 1 1) surface in the acidic solution (pH 0.3) can be obtained by the long-term potentiostatic polarization at 0.6–0.9 V (the degree of activation depends on the potential and duration of treatment, see details in Refs. [15,28–30]). Curve 1 in Fig. 6b corresponds to the steady-state CV at a sweep rate 0.1 V s^{-1} (the polarization routine is illustrated in the insert to Fig. 6b). The first cycle after the electrode exposure at a potential of 0.8 V for 500 s (curve 2) indicates both the acceleration of Cu UPD (peak at 0.59 V) and the adlayer desorption at less positive potentials due to the formation of copper oxides during the delay [30]. Cycling the potential for 15–20 min leads to a gradual decrease in concentration of Cu_xO with time and the re-establishment of the steady-state CV profile (curve 1 in Fig. 6b).

It should be noted that cathodic profiles of curve 2 in Fig. 6b (activated Pt surface, pH 0.3) and steady-state CVs 2 and 3 in Fig. 2 (enhanced concentrations of adsorbed OH^- ions and copper oxides are expected at pH 1.7–3.0) are quite similar. This fact can be considered as an additional proof of the oxides formation during the activation of Pt at pH 0.3.

The gradual decrease in the concentration of adlayer defects, copper oxides Cu_xO, with an increase in solution acidity leads to a positive shift of the anodic peak of adlayer desorption (pH 0.3–3.7, Figs. 2 and 3). The decrease in the height of the right cathodic peak at ca. 0.6 V (the formation of $(\sqrt{3} \times \sqrt{3})R30^\circ$) for pH variation from 2.7 to 0.3 is due to the decrease in the rate of copper ions reduction at $E > 0.55$ (Fig. 6), which depends on the adsorption of OH^- ions and the amount of Cu_xO.

However, the acceleration of Cu deposition at the stage of $(\sqrt{3} \times \sqrt{3})R30^\circ$ formation at the pH decrease from 3.7 to 3.0 (Figs. 2–4) is not so evident. It is well known that coadsorption lattice $(\sqrt{3} \times \sqrt{3})R30^\circ$ consists of two-thirds monolayer (ML) of Cu adatoms and one-third ML of bisulfate anions in acid solutions [8,9,46–52]. At the formation of a well-ordered adlayer at 0.5–0.6 V in solutions at pH 3.0–3.7, adsorbed hydroxide ions should be replaced for Cu atoms and

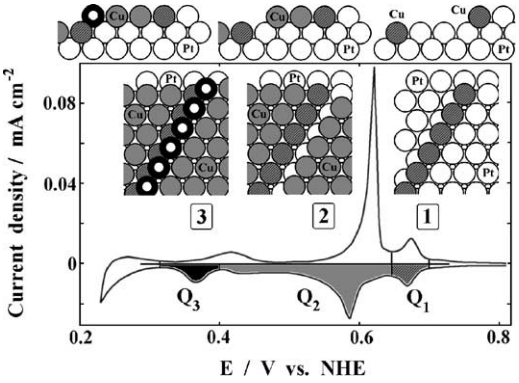

Fig. 7. CV of Pt(7 7 5) electrode at sweep rate of 5 mV s^{-1} in the acid solution (pH 0.3). The sketches show positions of Cu adatoms on the steps and terraces of Pt surface.

sulfate anions, the rate of the displacement evidently depends on the potential and concentration of OH-species. Thus, in the presence of high concentration of adsorbed oxygen compounds, the first stage of the UPD could be hindered, the decrease in OH^- adsorption at $E > 0.5$ V and the amount of copper oxides could accelerate $(\sqrt{3} \times \sqrt{3})R30^\circ$ formation.

To testify this hypothesis, we used a single crystal electrode Pt(7 7 5) with the stepped surface consisting of six-atomic width (1 1 1) terraces and (1 1 0) steps (Figs. 7 and 8). In the acidic copper sulfate solution (pH 0.3, Fig. 7), the first stage of Cu UPD is the one-dimensional decoration of steps at potentials 0.65–0.70 V [31,53]. The charge density $Q_1 \approx 0.08$ mC cm^{-2} of this process is about one-sixth of $Q_1 + Q_2 \approx 0.48$ mC cm^{-2}, which corresponds to Cu UPD on (1 1 1) terraces of the Pt(7 7 5) electrode at $E > 0.4$ V. At potentials 0.3–0.4 V, one-dimensional deposition of Cu takes place on stepped Pt atoms partially blocked by copper, $Q_3 \approx Q_1$. The adsorption energy of the latter process is lower than that of Cu UPD on the terraces, due to additional repulsion between neighboring positively charged Cu atoms. In the case of nine-atomic terraces of Pt(5 5 4) electrode the relation $Q_3 \approx (Q_1 + Q_2)/9 \approx Q_1$ is valid [31].

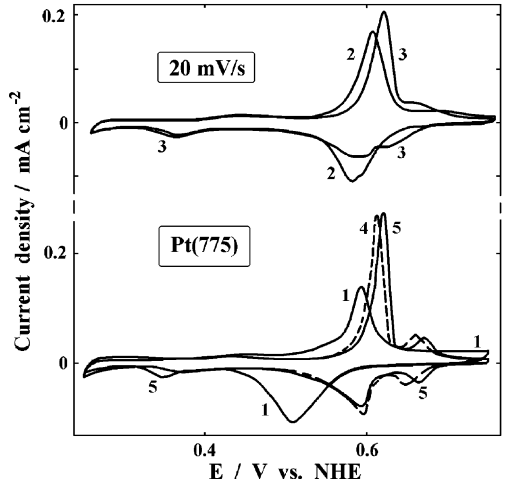

Fig. 8. CVs of Cu UPD on Pt(7 7 5) electrode at sweep rate of 20 mV s^{-1} in solutions of different acidities. pH values: 1–3.7; 2– 3.0; 3–2.6; 4–2.4; 5–2.1.

Steady-state CVs of Pt(7 7 5) in solutions at pH 2.75–3.7 for the sweep rates of 5–100 mV s^{-1} do not show any decoration of steps by Cu adatoms at $E > 0.6$ V (see, e.g., curves 1 and 2 in Fig. 8), the steps are blocked by adsorbed OH^- ions and/or copper oxides, although positive shifts of both anodic and cathodic peaks are observed with the decrease in pH (the experiment was started in the solution with pH 3.7, corresponding aliquots of 0.5 M H_2SO_4 were introduced directly to the cell to increase the acidity of the electrolyte). First indications of the one-dimensional decoration of steps at $E > 0.6$ V are observed at pH 2.6 (curve 3 in Fig. 8). At pH 2.1–2.4, the concentration of adsorbed oxygen-containing species is not very high, the processes of Cu deposition on the steps and Cu dissolution from the steps are almost reversible (curves 4 and 5 in Fig. 8) even at a relatively high sweep rate of 20 mV s^{-1}.

These data allow one to explain the acceleration of the first UPD stage $(\sqrt{3} \times \sqrt{3})R30^\circ$ formation, on Pt(1 1 1) electrode with the pH decrease from 3.7 to 2.7 (Figs. 2–4). Probably, at $E > 0.55$ V and pH > 3.0, the process of formation of the ordered $(\sqrt{3} \times \sqrt{3})R30^\circ$ lattice is controlled by desorption of oxygen-containing species from the steps and terraces. In solutions with higher acidity (pH < 2.7), the decrease in UPD rate at potentials 0.5–0.6 V could be caused by the lower charge transfer rates due to the weaker adsorption of hydroxide ions (Fig. 5). It is important to note, that optimal, not very high, concentrations of adsorbed oxygen-containing species are necessary for ensuring the maximum rate of Cu UPD on platinum (pH 2.7–3.0).

The formation of a complete monolayer of Cu_{ad} on the Pt(1 1 1) surface at pH 3.7 occurs at more positive potentials (curve 1 in Figs. 2–4) and the adlayer desorption takes place at less positive potentials as compared with other studied solutions. Adsorption of hydroxide ions and formation of copper oxides ensure the high concentration of active centers (adlayer defects) for both the two-dimensional phase transition of $(\sqrt{3} \times \sqrt{3})R30^\circ$ lattice to a Cu(1 × 1) monolayer and the Cu_{ad} desorption.

In contrast to Cu UPD on Pt(poly), where super-monolayer deposition with $\theta_{Cu} = 1.7$ ML was observed at pH 3.7 [15], the surface coverage of copper on Pt(1 1 1) in solutions of different acidities is about 1 ML at $E = 0.25$ V (Fig. 4). Probably, an adlayer with $\theta_{Cu} > 1$ ML could be formed on another faces of Pt(*h k l*) [54].

3.2. Potentiostatic current transients of Cu OPD on Pt(1 1 1)

3.2.1. Kinetics of Cu deposition at pH 0.3 and 3.7

Our previous studies have shown that electrochemical pretreatment and electrolyte acidity affect the rate of bulk copper deposition on Pt(poly) [14–16,27,29,57]. Some data on the Cu OPD on Pt(1 1 1) electrode were presented in Ref. [30].

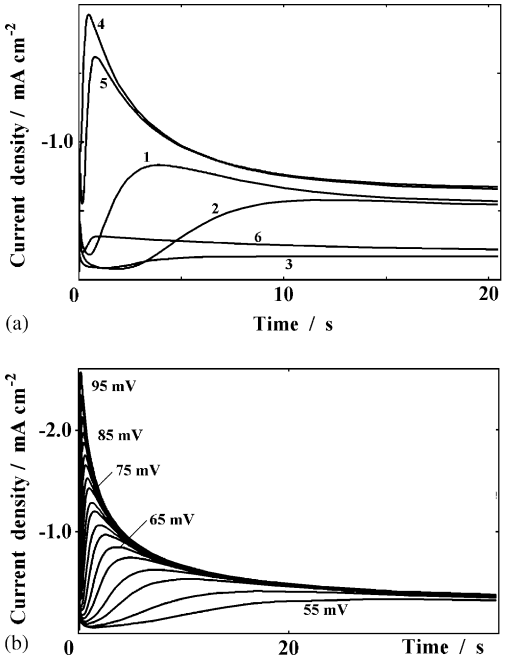

Fig. 9. Potentiostatic current transients of Cu deposition on Pt(1 1 1) electrode: (a) (1, 2, 4 and 5) pH 3.7; (3 and 6) pH 0.3. Cathodic overpotentals: (1–3) 60 mV; (4–6) 80 mV. (b) pH 3.7; the overpotentals are pointed near the curves. Details of electrochemical pretreatment are described in the text.

This section is devoted to kinetics of bulk copper deposition on Pt(1 1 1) in solutions of different acidities (pH 0.3–3.7).

Potentiostatic current transients of Cu deposition at pH 3.7 and 0.3 are shown in Fig. 9. Curves 1, 3, 4 and 6 in Fig. 9a and transients in Fig. 9b were recorded at cathodic overpotentials applied after potential cycling at 0.1 V s^{-1} and the subsequent polarization at 0.25 V for 10 s (this period of time is long enough for stabilization of the adlayer structure). Curves 2 and 5 in Fig. 9a were obtained at pH 3.7 after cycling and a 500 s exposure at 0.25 V, in this case cathodic currents of Cu deposition are lower as compared with the short-time polarization at 0.25 V in the same solution (curves 1 and 4). Similar inhibition effect we observed in acid solution [30] due to the reduction of copper oxides (active centers of both UPD and OPD processes) at low potentials. The data in Fig. 9a show that the kinetics of Cu nucleation and growth on Pt(1 1 1) in weakly acidic solution can be controlled by electrochemical pretreatment. Polarization at 0.25 V does not modify the surface structure of the electrode; the amount of structural defects (steps of (1 1 1) terraces, active centers of nucleation) should not depend on the duration of this pretreatment. We see the only explanation for the decrease in Cu deposition rate after the long-term treatment at 0.25 V (curves 2 and 4 in Fig. 9a), the decrease in the number of active centers due to the reduction of adsorbed copper oxides. Probably, in the vicinity of these species, the formation of a critical nucleus and/or growth of a Cu crystallite proceed at higher rates (accelerated charge transfer) as compared with the ordered monolayer of Cu(1 × 1).

The transients 3 and 6 in Fig. 9a were recorded at pH 0.3, Pt(1 1 1) electrode was pretreated by potential cycling in the range of 0.25–1.0 V, followed by 10 s exposure at 0.25 V. The rate of Cu deposition in the acid solution is notably lower than that at pH 3.7 (Fig. 9). This is due to the small number of active centers (copper oxides) and a slow copper ions reduction (Fig. 5).

In order to estimate the kinetic parameters of Cu nucleation, a popular model [58] for the diffusion-controlled growth of nuclei was applied, it makes it possible to calculate the nucleation rate J_1 and the number of active centers N_0 by using the following equation for current density:

$$I(t) = SzFDC(\pi Dt)^{-1/2} \times \left[1 - \exp\left\{-\pi N_0 k D t \left(1 - \frac{[1 - \exp(-J_1 t)]}{J_1 t}\right)\right\}\right]$$

where $k = (8\pi C V_a)^{1/2}$, C the concentration of electroactive ions, D the diffusion coefficient, z the charge, F the Faraday constant, V_a the atomic volume, S is the surface area of the electrode.

Overpotential dependencies of N_0, J_1 and the total nucleation rate $J_0 = N_0 J_1$ are shown in Fig. 10a in semi-logarithmic coordinates for the data gained in a weakly acidic solution (pH 3.7, Fig. 9b). These values were calculated using the parameters of transient maxima I_m and t_m, then N_0 and

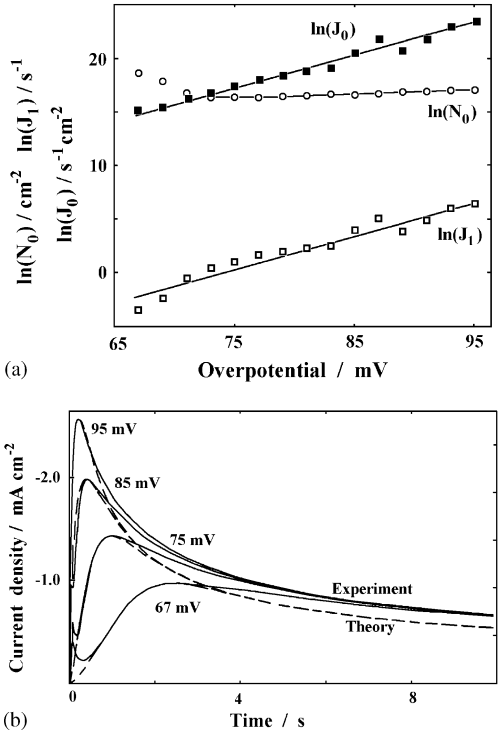

Fig. 10. (a) The results of processing the current-transient maxima (the data in Fig. 9b) in accordance with the model [58]. (b) Experimental (solid lines) and simulated (dashed lines) current transients of Cu deposition on Pt(1 1 1) electrode in solution of 0.5 M Na_2SO_4 + 0.5 mM H_2SO_4 + 10 mM $CuSO_4$ (pH 3.7). Cathodic overpotentals are pointed near the curves.

J_1 were applied for simulation of model curves (Fig. 10b). The slope of $\ln(J_1) - \eta$ dependence (Fig. 10a) corresponds to the size of critical nucleus of three to four atoms to the first approximation [62–65]. The diffusion coefficient of $D = 1.8 \times 10^{-6}$ cm^2 s^{-1} was used as an effective parameter; this value of D allows one to process most of current transients shown in Fig. 9b ($\eta > 65$ mV) in accordance with the model [58], however, it is lower than the table value of 8×10^{-6} cm^2 s^{-1}. According to the theory [58] developed for diffusion controlled growth of hemispherical nuclei, the calculation is only possible if the relationship $0.7153 < (I_m/zFC)(\pi t_m/D)^{0.5} < 0.9034$ is fulfilled, the values 0.7153 and 0.9034 correspond to the limiting cases of instantaneous and progressive nucleation, respectively. Using the table value of $D = 8 \times 10^{-6}$ cm^2 s^{-1}, we can calculate the nucleation rate and the number of active sites only for cathodic overpotentials higher than 85 mV, these conditions better correspond to the diffusion control of the deposition, at lower overpotentials the growth of Cu crystallites is controlled by both charge transfer kinetics and diffusion of copper ions with a high contribution of the charge transfer. Using the lowered value of D for calculating the nucleation parameters, we keep in mind that the model used does not describe properly the experimental system with mixed control over the growth, the obtained values of N_0 and J_1 could be only considered as a rough approximation. Processing the data by means of similar models [59–61] leads to the same conclusions.

A comparison of simulated and experimental transients for several overpotentials (Fig. 10b) gives satisfactory agreement in the vicinity of maxima but experimental currents for $t > t_m$ are higher than theoretical ones for the diffusion controlled growth. The discrepancy between the theory and experimental data (including the smaller value of diffusion coefficient used for the calculation) is due to the growth of a copper deposit under the mixed control "diffusion + charge transfer" for the system studied (this point was discussed in detail for Cu OPD on Pt(poly) in Refs. [16,57]).

Only a few of current transients recorded in the acid solution (pH 0.3) at overpotentials 30–150 mV could be processed by the theory [58] for the value of effective diffusion coefficient of ca. 0.2×10^{-6} cm^2 s^{-1} to evaluate the nucleation parameters. This is due to the higher contribution of charge transfer kinetics to the growth rate under the mixed control (see the effect of rotation speed on the rate of Cu deposition in Fig. 5). A comparison of theoretical and experimental curves at pH 0.3 was performed in Ref. [30], the discrepancy is substantially greater than that in the case of weakly acidic solution.

3.2.2. Morphology of deposits

Another reason for the discrepancy (Fig. 10b) is as follows. The theory [58] considers the nucleation and diffusion-controlled growth of hemispherical crystallites but this condition is not fulfilled in the case of Cu deposition on Pt(1 1 1) in acid solution. Fig. 11 shows the scanning electron microscopy (SEM) image of the copper deposit (pH 0.3, ca. 500 effective monolayers), the layer-by-layer growth dominates at low overpotentials with the formation of an epitaxial pseudomorphic deposit. Under these conditions, one should not expect any good correlation between the models [58–61] and the system studied.

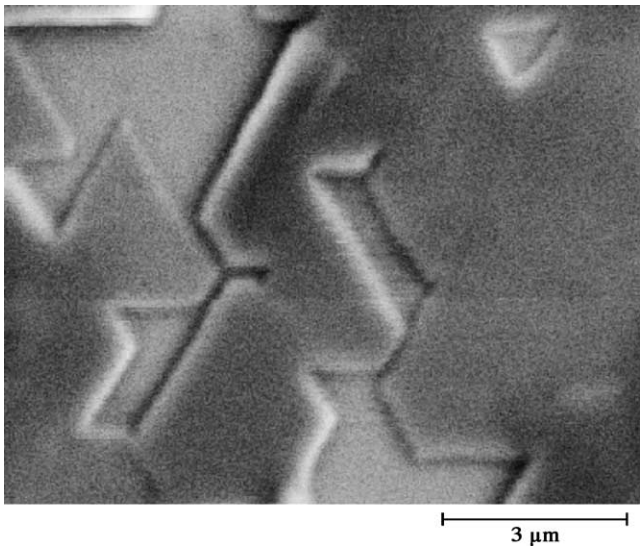

Fig. 11. Morphology of Cu deposit on Pt(1 1 1) electrode obtained in solution of 0.5 M H_2SO_4 + 10 mM $CuSO_4$ (pH 0.3) at overpotental $\eta = 70$ mV for ca. 30 min (approximately 500 effective monolayers, SEM image).

We failed to gain high quality SEM images of copper deposited on Pt(1 1 1) at pH 3.7, we observed very flat surfaces without any characteristic features. To analyze the morphology at initial stages of the deposition, ex situ STM study was performed. The electrode was pretreated in a usual way, copper was deposited at overpotentials 50–100 mV for 50 s and current transients were recorded, then, the meniscus was broken and the electrode was rinsed with Milli-Q water, dried with argon and transferred to STM in air. STM images were obtained with tungsten etched tips at a bias voltage of 50–100 mV and a tunneling current of 0.5–1.0 nA.

At high overpotentials, the deposits consist of separate crystallites with the lateral size much greater than the height (STM images in Fig. 12). There is no principle difference in the morphology of deposits obtained in solutions at pH 0.3 and 3.7. However, the number of crystallites at $\eta = 75$ mV is higher at pH 3.7 as compared with pH 0.3 (images a and b), this is an indication of the enhanced number of active centers in the weakly acidic solution.

3.2.3. Kinetics of Cu deposition at intermediate pH

To estimate the kinetics of Cu deposition at intermediate pH 0.3–3.7, a series of current transients were recorded after the potential cycling in the ranges 0.25–E_a at a sweep rate of 0.1 V s^{-1} and the potentiostatic treatment at 0.25 V for 0.5 s ($E_a = 0.75$ V at pH 3.0–3.7, $E_a = 0.85$ V at pH 1.0–2.7, $E_a = 0.90$ V at pH 0.3). Fig. 13a shows the transients for cathodic overpotenial $\eta = 70$ mV in solutions of different acidities. Results of integration of the I, t-curves (cathodic

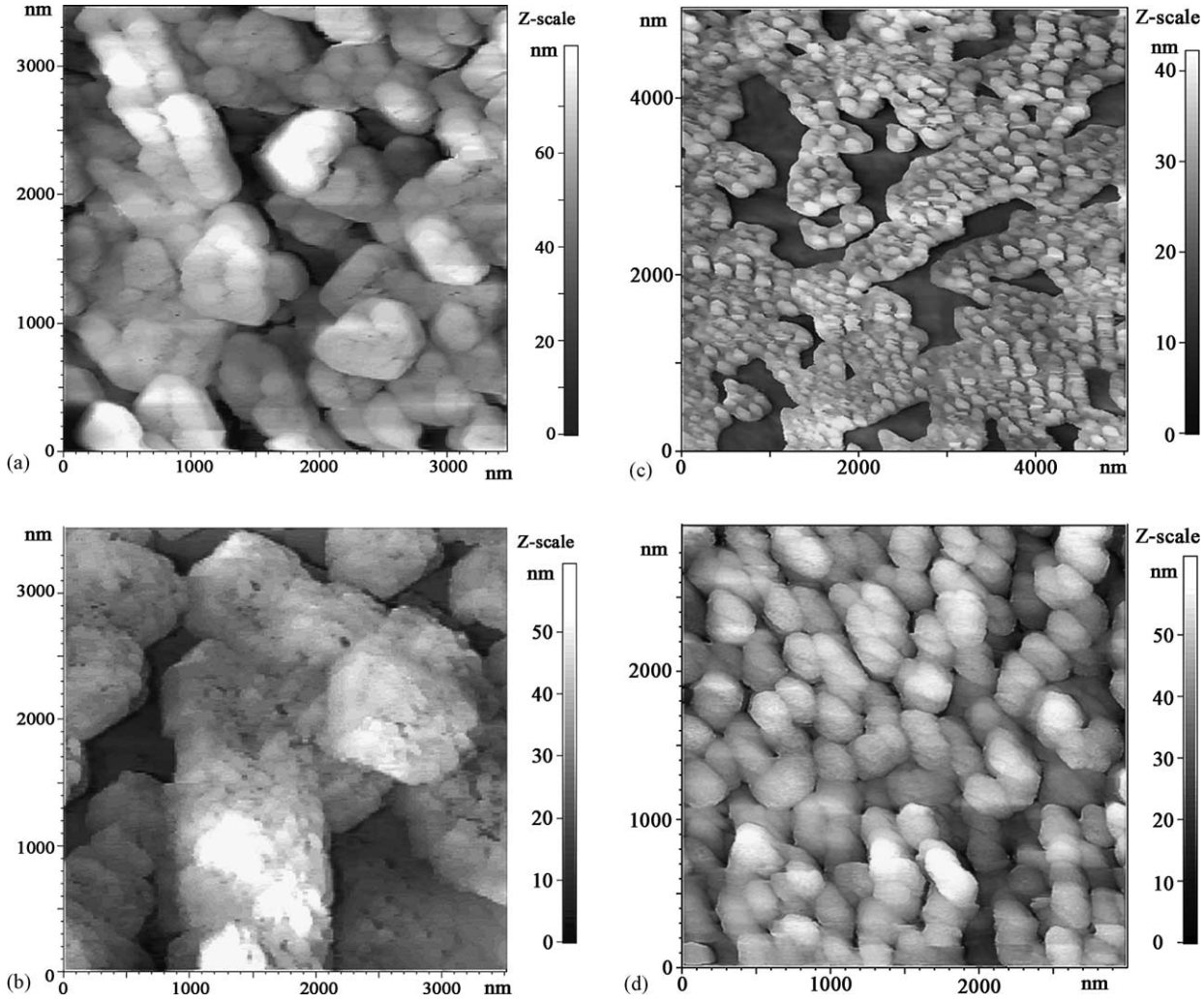

Fig. 12. Ex situ STM images of Cu deposits on Pt(1 1 1) electrode obtained in solutions of: (a) 0.5 M Na_2SO_4 + 0.5 mM H_2SO_4 + 10 mM $CuSO_4$ (pH 3.7), deposition at η = 75 mV for 50 s; (b–d) 0.5 M H_2SO_4 + 10 mM $CuSO_4$ (pH 0.3), deposition at η = 75 mV (b) and 100 mV (c and d) for 50 s. *Z*-scales are shown to the right of the images.

charges Q_c for 50-s Cu deposition at η = 40–200 mV) are presented in Fig. 13b as a function of the overpotenial for different pH. The transients for pH 1.7 and η = 50–200 mV are plotted in Fig. 14.

Curves 1–6 in Fig. 13a show that the increase in acidity of solutions (pH 1.0–3.7) inhibits the nucleation at η = 70 mV (a decrease of the maximum height I_m and an increase of t_m) due to the decrease in the number of active centers (copper oxides) and the lower rate of copper ions discharge, a similar effect is observed at higher overpotentials. At pH 3.7 and η > 100 mV, only a slight increase in Q_c is observed (Fig. 13b), the deposition is diffusion-controlled to a considerable extent due to the high rate of charge transfer (Fig. 5).

In the acid solution (pH 0.3), the t_m value is smaller than that at pH 1.0–3.2 but I_m is very low (Fig. 13a). This indicates the formation of a relatively high concentration of crystallization centers and their slow growth. The number of nuclei (Fig. 12b–d), the rate of charge transfer (Fig. 5) and values of Q_c (Fig. 13b) increase with overpotential, the mixed kinetics controls the growth of copper crystallites as was pointed above.

At intermediate acidity of solutions, a surprising feature is that the Q_c,η dependence has a maximum at η = 100–110 mV (Fig. 13b), this effect is well-defined for pH 1.7. To our knowledge, this phenomenon has not been described in the literature previously. In contrast to the data in Fig. 9, the transients at pH 1.7 and overpotentials of 60–200 mV intersect (Fig. 14). This is the case, when the control of metal deposition at different overpotentials is not the same, the contribution of charge transfer kinetics to the mixed control "diffusion + discharge" is higher at low η and lower at high η. The nucleation rate and the number of nuclei should increase with overpotential (the height of the maximum, I_m, increases and t_m decreases), however, the rate of deposit growth at t > 25 s (cathodic current) is the highest for intermediate overpotentials η = 80–100 mV.

The applied potential determines the number of nuclei, the average distance between crystallization centers, the rate of charge transfer (rate of Cu^{2+} ions consumption at small times)

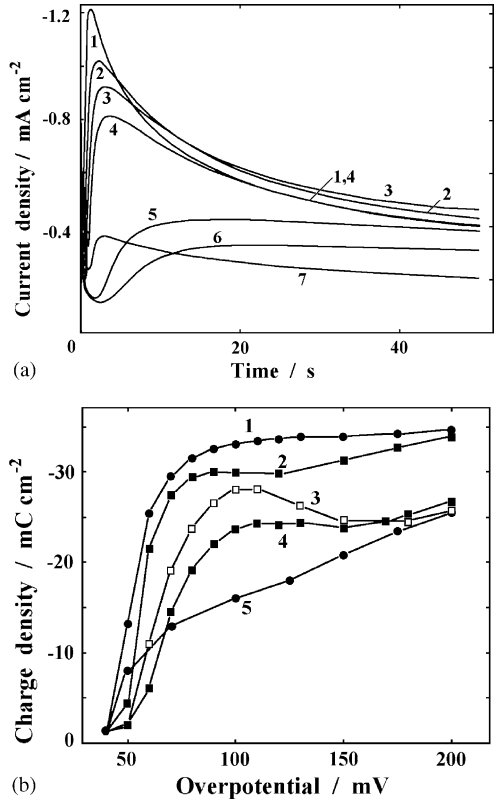

Fig. 13. (a) Current transients of Cu deposition at cathodic overpotential 70 mV in solutions of different acidities. pH values: 1–3.7; 2–3.4; 3–3.2; 4–3.0; 5–1.7; 6–1.0; 7–0.3. (b) Dependencies of deposited Cu amount on the cathodic overpotential in solutions of different acidities. pH values: 1–3.7; 2–3.0; 3–1.7; 4–1.0; 5–0.3.

and consequently, the moment, when diffusion control begins to play a decisive role in the growth kinetics (a decrease in current density is observed).

Probably, at $\eta > 110$ mV, fast nucleation leads to the formation of a large number of copper nuclei, diffusion zones of reduced Cu^{2+} concentration overlap one another at short times and the further relatively slow growth proceeds mainly under the diffusion control (close to Cottrell's

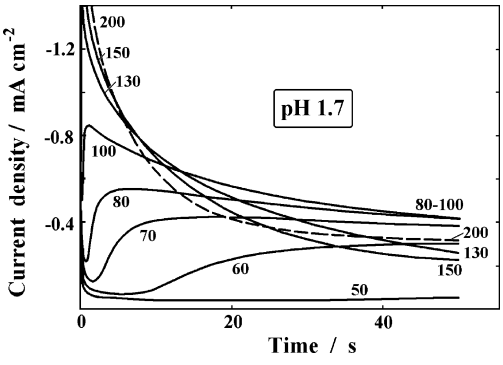

Fig. 14. Series of the current transients for Cu deposition on Pt(1 1 1) electrode in solution of 0.45 M Na_2SO_4 + 0.05 M H_2SO_4 + 10 mM $CuSO_4$ (pH 1.7). Cathodic overpotentals are pointed near the curves.

conditions). At η = 90–100 mV, the growth of a smaller number of crystallization centers (the average distance between crystallites is greater) proceeds under a relatively fast mixed control for a more extended time thus the overlapping of zones occurs later. In this case the amount of deposit could exceed that obtained at higher overpotentials if the deposition was not too short-term. To analyze this phenomenon in detail, the STM studies and numerical modeling are in a progress.

As a conclusion of this section, it is worth noting the correlation between the activity of Pt(1 1 1) surface with respect to Cu UPD and OPD processes in solutions of different acidities. In weakly acidic solutions, the rates of both Cu UPD and OPD processes are higher due to the enhanced concentration of active centers for two- and three-dimensional phase transitions (copper oxides Cu_xO or mixed oxides Cu_xPt_yO) and the accelerated discharge of copper ions.

3.3. Cyclic voltammetry, Cu UPD and OPD on Au(1 1 1)

After controlling the cleanness of the system and the quality of crystals in sulfuric acid, the electrode was transferred to the cell with acid copper sulfate (pH 0.3, the upper limit of potential cycling E_a = 1.3 V) or with weakly acid solution (pH 3.7, E_a = 1.1 V). In contrast to Pt(1 1 1) electrode, the positions of sharp peaks A_2 and D_2 at ca. 0.5 V (formation and destruction of the lattice $(\sqrt{3} \times \sqrt{3})R30^\circ$ [46–52]) in solutions of different activity for Au(1 1 1) are almost the same (Fig. 15) due to the lower adsorption of hydroxide ions on gold [66]. A small positive shift of these peaks in the weakly acidic solution could be due to the enhanced coadsorption of copper adatoms and anions SO_4^{2-} and OH^- whose adsorption at pH 3.7 is stronger as compared with HSO_4^- anions at pH 0.3.

Potential cycling was combined with potentiostatic polarization at various potentials. No noticeable activation effects were observed on Au(1 1 1) in acid solution (pH 0.3) after long-term (500 s) treatment at E_h = const. It is worth noting a sharp boundary of potential ranges (the potential between 0.29 and 0.30 V) of the existence of two-dimensional phases $(\sqrt{3} \times \sqrt{3})R30^\circ$ and Cu(1 × 1) at pH 0.3. In weakly acidic solution, the formation of a complete monolayer takes place in wider range of potentials 0.3–0.4 V. This is probably due to the changes in anion adsorption, the honeycombs of the lattice $(\sqrt{3} \times \sqrt{3})R30^\circ$ could be occupied by strongly bonded SO_4^{2-} and OH^- ions at pH 3.7 in place of bisulfate anions at pH 0.3.

The integration of positive-going sweeps (from E_h to 0.8 V without double layer correction) recorded immediately after potentiostatic polarization at various potentials E_h for 500 s gives isotherms of Cu adatoms adsorption (Fig. 16, curves 3 and 4) to the first approximation. Dynamic isotherms of Cu adsorption on Au(1 1 1) electrode were obtained by integrating negative-going sweeps of steady-state CVs from 0.8 to 0.25 V (sweep rate of 0.1 V s^{-1}, absolute values of charge densities are plotted, curves 1 and 2 in Fig. 16). The dynamic

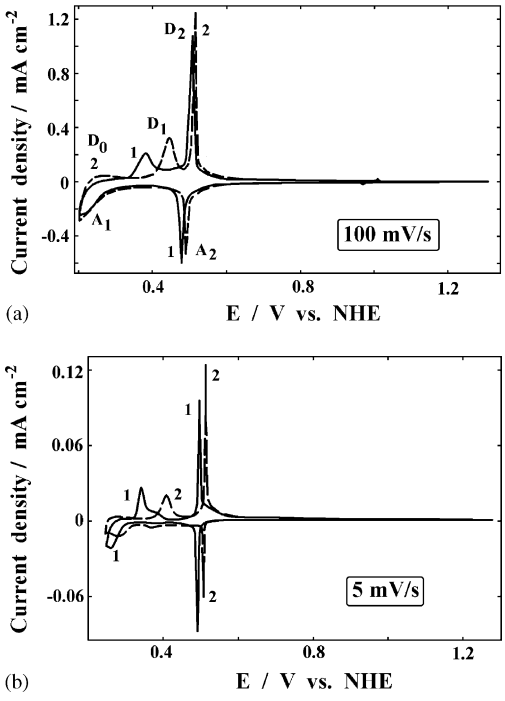

Fig. 15. Steady-state CV profiles of Au(1 1 1) electrode in solutions of 0.5 M H_2SO_4 + 10 mM $CuSO_4$ (1, pH 0.3) and 0.5 M Na_2SO_4 + 0.5 mM H_2SO_4 + 10 mM $CuSO_4$ (2, pH 3.7) at sweep rates of: (a) 100 mV s^{-1} and (b) 5 mV s^{-1}.

isotherms of Cu adsorption on Pt(1 1 1) electrode (curves 5 and 6 in Fig. 16) are also shown for a comparison.

One can see that the rate of Cu UPD on Au(1 1 1) electrode is considerably slower than that on Pt(1 1 1) under conditions of potential cycling at a sweep rate of 100 mV s^{-1} (curves 1, 2, 5 and 6 in Fig. 16). In addition to different energies of interatomic Pt–Cu and Au–Cu interactions [67,68], another possible reason for this phenomenon could be low adsorption of oxygen-containing species on gold.

In contrast to the Cu UPD on Pt(1 1 1), on Au(1 1 1) electrode one can observe (Fig. 16):

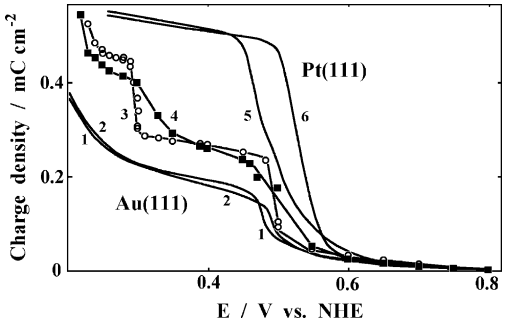

Fig. 16. Steady-state (symbols, curves 3 and 4, 500 s exposure at E_h = constant) and dynamic (sweep rate of 0.1 V s^{-1}, curves 1, 2, 5 and 6) isotherms of Cu_{ad} on Au(1 1 1) (1–4) and Pt(1 1 1) (5 and 6) electrodes in solutions of 0.5 M H_2SO_4 + 10 mM $CuSO_4$ (pH 0.3, curves 1, 3 and 5) and 0.5 M Na_2SO_4 + 0.5 mM H_2SO_4 + 10 mM $CuSO_4$ (pH 3.7, curves 2, 4 and 6).

(i) a very small difference in the kinetics of Cu deposition in solutions with pH 0.3 and 3.7 (curves 1 and 2);
(ii) the Cu surface coverage at the potentials 0.26–0.3 V and 0.40–0.45 V at pH 3.7 is less than that in acid solution (curves 3 and 4);
(iii) a sharp increase in the Cu surface coverage with a decrease in potential (separated potential ranges of the existence of the Cu(1 × 1) layer and the $(\sqrt{3} \times \sqrt{3})R30^\circ$ lattice) in acid solution (curve 3) and smooth changes in the Cu coverage with potential at pH 3.7 (curve 4).

Summarizing these findings, we have to stress the important role of anions adsorption in the kinetics and thermodynamics of UPD processes. Low adsorption of OH^- ions on gold at $E > 0.5$ V and induced OH^- adsorption in the presence of Cu adatoms at $E < 0.5$ V allows us to explain the experimental data presented above. At the stage of $(\sqrt{3} \times \sqrt{3})R30^\circ$ formation (Fig. 15), a part of bisulfate or sulfate anions could be replaced for hydroxide ions. In this case, negatively charged oxygen species are in a contact with positively charged atoms of gold and especially, copper, the replacement of OH^- ions for Cu atoms at more negative potentials could proceed more slowly than that of bisulfate anions due to the strong lateral interaction between oxygen and copper in the plane of the adlayer.

Fig. 15b shows CVs of Cu UPD on Au(1 1 1) recorded at 5 mV s^{-1}. Similar data have been reported in Ref. [12]. At this sweep rate, a complete Cu(1 × 1) monolayer forms in both solutions in the underpotential region. The more positive potential of the desorption peak D_1 for the phase transition "Cu(1 × 1)–$(\sqrt{3} \times \sqrt{3})R30^\circ$" in weakly acidic solution deserves mention (see also Fig. 15a). Probably, this is due to the stronger stabilizing action of sulfate and hydroxide ions as compared with bisulfate anions, which are placed on the monolayer of copper adatoms.

To estimate a rate of bulk copper deposition on gold in solutions of different acidities, the CVs with various cathodic limits were recorded at a sweep rate of 0.1 V s^{-1}. The anodic peak D_0 corresponds to the dissolution of three-dimensional (3-D) Cu crystallites, it is observed after potential excursions to 0.20 V or less positive potentials in weakly acidic solution (Fig. 15a) and to $E \leq 0.16$ V in acid solution. It means that 3-D nucleation at pH 3.7 proceeds faster at more positive potentials.

The influence of the solution acidity on the amount of deposited copper is clearly seen in Fig. 17, where CVs in the same potential ranges (cathodic limits E_c = 0.13 and 0.11 V, respectively) are plotted together for a comparison. During the negative-going sweeps in the range of 0.25–0.45 V (the formation of an adatomic layer), the cathodic currents are practically pH-independent, while at less positive potentials, the accelerated bulk copper deposition with noticeable "nucleation loops" is observed in weakly acid solution. The nucleation loops for CVs with E_c = 0.13 V (Fig. 17a) and

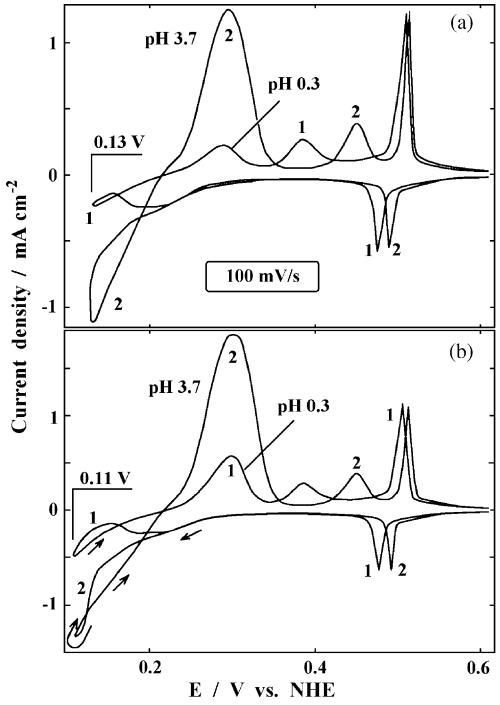

Fig. 17. CV profiles of: (a) Au(1 1 1) electrode in solutions of 0.5 M H_2SO_4 + 10 mM $CuSO_4$ (pH 0.3) and (b) 0.5 M Na_2SO_4 + 10 mM $CuSO_4$ (pH 3.7) at sweep rate of 0.1 V s^{-1}. Cathodic limits of cycling are indicated near the curves.

curve 1 in Fig. 17b are typical of metal deposition under the kinetic control [29], however, the CV profile in weakly acidic solution for $E_c = 0.11$ V (curve 2 in Fig. 17b) indicates the mixed control of nuclei growth, because after the reversal of potential sweeping the cathodic current is lowered due to the contribution of diffusion control. At the potentials 0.13–0.18 V, the cathodic current of positive-going sweep is higher again than that of the cathodic sweep due to the higher surface area of growing deposits (curve 2 in Fig. 17b). A change in the current sign takes place at ca. 0.25 V (Cu^{2+}/Cu equilibrium potential) at positive-going sweeps, the integration of anodic peaks D_0 from 0.25 to 0.35 V (Fig. 17a) gives the approximate amount of bulk copper deposits, viz., 0.3 and 2 effective monolayers (EML) for pH 0.3 and 3.7, respectively. Similar calculations for the CVs shown in Fig. 17b ($E_c = 0.11$ V) give 0.6 EML for pH 0.3 and 3 EML of bulk Cu on Au(1 1 1) for pH 3.7.

High rates of metal deposition are observed usually, when: (i) a large number of active sites are available for 3-D nucleation on the substrate and (ii) the rate of charge transfer is high enough. In the case of bulk copper deposition on Au(1 1 1) in weakly acidic solution (pH 3.7), both these factors probably play a role. Adsorption of hydroxide ions during the formation of $(\sqrt{3} \times \sqrt{3})R30^\circ$ and Cu(1 × 1) could give rise to the centers, in which the nucleation and growth of bulk copper proceeds faster and facilitate the initial stages of the overpotential deposition under accelerated discharge of copper ions (Fig. 5).

4. Conclusions

(1) Although the bulk concentration of OH^- ions is very low in weakly acidic solutions, the adsorption of hydroxide ions on the Pt(1 1 1) surface and a Cu(1 × 1) monolayer could be high enough to ensure the formation of chemisorbed copper oxides Cu_xO or mixed oxides Pt_xCu_yO, which are the active sites of the Cu UPD process.

(2) There is a correlation between the activity of Pt(1 1 1) surface with respect to Cu UPD and OPD processes in solutions of different acidities. In weakly acidic solutions, the rates of both Cu UPD and OPD processes are higher as compared with acid solution of copper sulfate (pH 0.3) due to the higher concentration of active centers for two- and three-dimensional phase transitions (copper oxides Cu_xO or mixed oxides Cu_xPt_yO) and the accelerated discharge of copper ions.

(3) The maximum rate of $(\sqrt{3} \times \sqrt{3})R30^\circ$ formation is observed at pH 2.7–3.0. At pH > 3.0, the platinum surface is partially blocked by strongly adsorbed oxygen-containing species. At pH < 2.7, the inhibition of Cu UPD and the adlayer desorption are due to the decrease in charge-transfer rate and concentration of copper oxides and also defects of the adlayer. An optimal, not very high, concentration of adsorbed oxygen-containing species is necessary for ensuring the maximum rate of Cu UPD on platinum.

(4) Acidity of the electrolytes studied (pH 0.3–3.7) considerably affects the rate of Cu deposition on Pt(1 1 1) but has only a slight influence on the kinetics of Cu adlayer formation on the Au(1 1 1) electrode due to the different adsorption of OH^- ions on Pt and Au substrates. The first stage of Cu monolayer desorption (phase transition Cu(1 × 1)–$(\sqrt{3} \times \sqrt{3})R30^\circ$) on gold is hindered in weakly acidic solution as compared with acid one, this is probably due to stabilization of the Cu(1 × 1) monolayer by adsorbed sulfate anions and hydroxide ions.

(5) The increase in pH accelerates bulk Cu deposition on Au(1 1 1). The adsorption of sulfate anions and hydroxide ions on a monolayer of copper adatoms and Cu crystallites provides an accelerated charge transfer (local electrostatic double layer effects of electronegative species) and probably increases the number of active centers for three-dimensional nucleation.

Acknowledgements

The study was supported by Russian Foundation for Basic Researches, Grants 01-03-32013 and 04-03-32326, the Council for Grants of President of the Russian Federation, Grant SciSch 658.2003.3 and Spanish MCyT, Project BQU2004-04209.

References

[1] D.M. Kolb, in: H. Gerischer, C.W. Tobias (Eds.), Advances in Electrochemistry and Electrochemical Engineering, vol. 11, NY, 1978, p. 125.
[2] K. Juttner, W.J. Lorenz, Z. Phys. Chem. N.F. 122 (1980) 163.
[3] R.R. Adzic, in: H. Gerischer (Ed.), Advances in Electrochemistry and Electrochemical Engineering, vol. 13, NY, 1984, p. 159.
[4] G. Kokkinidis, J. Electroanal. Chem. 201 (1986) 217.
[5] A. Aramata, in: J.O.'M. Bockris (Ed.), Modern Aspects of Electrochemistry, vol. 31, Plenum Press, NY, 1997, p. 181.
[6] A.I. Danilov, Russ. Chem. Rev. 64 (1995) 767.
[7] A. Wieckowski, K. Itaya (Eds.), Proceedings of the Sixth International Symposium on Electrode Processes, The Electrochemical Society Proceedings, vol. 96–8, 1996.
[8] A. Wieckowski (Ed.), Interfacial Electrochemistry: Theory, Experimental, and Applications, Marcel Dekker, NY, 1999.
[9] E. Herrero, L.J. Buller, H.D. Abruna, Chem. Rev. 101 (2001) 1897.
[10] T.I. Lezhava, K.G. Meladze, Sov. J. Electrochem. 14 (1978) 1651.
[11] A. De Agostini, E. Schmidt, W.J. Lorenz, Electrochim. Acta 34 (1989) 1243.
[12] M.H. Holzle, V. Zwing, D.M. Kolb, Electrochim. Acta 40 (1995) 1237.
[13] A.I. Danilov, E.B. Molodkina, Yu.M. Polukarov, Russ. J. Electrochem. 33 (1997) 288.
[14] A.I. Danilov, E.B. Molodkina, Yu.M. Polukarov, Russ. J. Electrochem. 36 (2000) 987.
[15] A.I. Danilov, E.B. Molodkina, Yu.M. Polukarov, Russ. J. Electrochem. 36 (2000) 976.
[16] A.I. Danilov, E.B. Molodkina, Yu.M. Polukarov, Russ. J. Electrochem. 36 (2000) 1092.
[17] H.D. Abruna, J.M. Feliu, J.D. Brock, L.J. Buller, E. Herrero, J. Li, R. Gomez, A. Finnefrock, Electrochim. Acta 43 (1998) 2899.
[18] R. Gomez, J.M. Feliu, H.D. Abruna, J. Phys. Chem. 98 (1994) 5514.
[19] N.M. Markovic, H.A. Gasteiger, P.N. Ross Jr., Langmuir 11 (1995) 4098.
[20] M.H. Holzle, U. Retter, D.M. Kolb, J. Electroanal. Chem. 371 (1994) 101.
[21] H. Matsumoto, I. Oda, J. Inukai, M. Ito, J. Electroanal. Chem. 356 (1993) 275.
[22] H. Matsumoto, J. Inukai, M. Ito, J. Electroanal. Chem. 379 (1994) 223.
[23] Y.-E. Sung, S. Thomas, A. Wieckowski, J. Phys. Chem. 99 (1995) 13513.
[24] I.M. Tidswell, C.A. Lucas, N.M. Markovic, P.N. Ross, Phys. Rev. B 51 (1995) 10205.
[25] J.H. White, H.D. Abruna, J. Phys. Chem. 94 (1990) 894.
[26] R. Gomez, H.S. Yee, G.M. Bommarito, J.M. Feliu, H.D. Abruna, Surf. Sci. 335 (1995) 101.
[27] A.I. Danilov, J.E.T. Andersen, E.B. Molodkina, Yu.M. Polukarov, P. Moller, J. Ulstrup, Electrochim. Acta 43 (1998) 733.
[28] A.I. Danilov, E.B. Molodkina, Yu.M. Polukarov, Russ. J. Electrochem. 34 (1998) 1257.
[29] A.I. Danilov, E.B. Molodkina, Yu.M. Polukarov, Russ. J. Electrochem. 36 (2000) 998.
[30] A.I. Danilov, E.B. Molodkina, Yu.M. Polukarov, V. Climent, J. Feliu, Electrochim. Acta 46 (2001) 3137.
[31] A.I. Danilov, E.B. Molodkina, A.V. Rudnev, Yu.M. Polukarov, J. Feliu, E. Herrero, V. Climent, Abstracts of 55th Annual Meeting of ISE, vol. 1, September 19–24, 2004, Thessaloniki, Greece, p. 41.
[32] H.Y.H. Chan, C.G. Takodius, M.J. Weaver, J. Phys. Chem. B 103 (1999) 357.
[33] B.J. Cruickshank, D.D. Sneddon, A.A. Gewirth, Surf. Sci. 281 (1993) L308.
[34] J.R. LaGraff, A.A. Gewirth, Surf. Sci. Lett. 326 (1995) L461.
[35] W. Li, R.J. Nichols, J. Electroanal. Chem. 456 (1998) 153.
[36] J. Clavilier, R. Faure, G. Guinet, R. Durand, J. Electroanal. Chem. 107 (1980) 205.
[37] J. Clavilier, J. Electroanal. Chem. 107 (1980) 211.
[38] J. Clavilier, D. Armand, S.G. Sun, M. Petit, J. Electroanal. Chem. 205 (1986) 267.
[39] J. Clavilier, in: A. Wieckowski (Ed.), Interfacial Electrochemistry: Theory, Experimental, and Applications, Marcel Dekker, NY, 1999, p. 231.
[40] A.M. Funtikov, U. Linke, U. Stimming, R. Vogel, Surf. Sci. Lett. 324 (1995) L343.
[41] A.M. Funtikov, U. Stimming, R. Vogel, J. Electroanal. Chem. 428 (1997) 147.
[42] A. Wieckowski, P. Zelenay, K. Varga, J. Chim. Phys. (Paris) 88 (1991) 1247.
[43] K.A. Jaaf-Golze, D.M. Kolb, D. Scherson, J. Electroanal. Chem. 200 (1986) 353.
[44] S. Taguchi, A. Aramata, J. Electroanal. Chem. 457 (1998) 73.
[45] N. Garcia, V. Climent, J.M. Orts, J.M. Feliu, A. Aldaz, Chem. Phys. Chem. 5 (2004) 1121.
[46] Z. Shi, J. Lipkowski, J. Electroanal. Chem. 365 (1994) 303.
[47] Z. Shi, S. Wu, J. Lipkowski, Electrochim. Acta 40 (1995) 9.
[48] Y.-E. Sung, S. Thomas, J.A. Tanzer, A. Wieckowski, in: A. Wieckowski, K. Itaya (Eds.), Proceedings of the Sixth International Symposium on Electrode Processes, The Electrochemical Society Proceedings, vol. 96–8, 1996, p. 28.
[49] M.F. Toney, J.N. Howard, J. Richer, G.L. Borges, J.G. Gordon, O.R. Melroy, Phys. Rev. Lett. 75 (1995) 4472.
[50] G. Nagy, T. Wandlowski, Langmuir 19 (2003) 10271.
[51] Y. Shingaya, H. Matsumoto, H. Ogasawara, M. Ito, Surf. Sci. 335 (1995) 23.
[52] Z.-L. Wu, Z.H. Zang, S.-L. Yau, Langmuir 16 (2000) 3522.
[53] C. Nishihara, N. Nozoye, J. Electroanal. Chem. 386 (1995) 75.
[54] L.A. Kibler, A. Cuesta, M. Kleinert, D.M. Kolb, J. Electroanal. Chem. 484 (2000) 73.
[55] T. Hachiya, H. Honbo, K. Itaya, J. Electroanal. Chem. 315 (1991) 275.
[56] Y. Shingaya, H. Matsumoto, H. Ogasawara, M. Ito, Surf. Sci. 335 (1995) 23.
[57] A.I. Danilov, E.B. Molodkina, A.A. Baitov, I.V. Pobelov, Yu.M. Polukarov, Russ. J. Electrochem. 38 (2002) 743.
[58] B.R. Scharifker, J. Mostany, J. Electroanal. Chem. 177 (1984) 13.
[59] M.V. Mirkin, A.P. Nilov, J. Electroanal. Chem. 283 (1990) 35.
[60] L. Heerman, A. Tarallo, J. Electroanal. Chem. 470 (1999) 70.
[61] L. Heerman, E. Matthijs, S. Langerock, Electrochim. Acta 47 (2001) 905.
[62] A. Milchev, Electrocrystallization, Fundamentals of Nucleation and Growth, Kluwer Academic Publishers, Boston, 2002.
[63] A. Milchev, S. Stoyanov, R. Kaischew, Thin Solid Films 22 (1974) 255.
[64] A. Milchev, E. Vassileva, V. Kertov, J. Electroanal. Chem. 107 (1980) 323.
[65] D. Kashchiev, J. Chem. Phys. 76 (1982) 5098.
[66] J. Mostany, J.M. Feliu, J. Lipkowski, J. Electroanal. Chem. 558 (2003) 19.
[67] E. Leiva, C. Sanchez, E.P.M. Leiva, Electrochim. Acta 45 (1999) 691.
[68] C. Sanchez, M.G. Del Popolo, E.P.M. Leiva, Surf. Sci. 421 (1999) 59.